

# Right/Left-Handed Transmission Lines Based on Coupled Transmission Line Sections and Their Application Towards Bandpass Filters

Jakub Sorocki, Ilona Piekarz, Krzysztof Wincza, *Member, IEEE*, and Sławomir Gruszczyński, *Member, IEEE*

**Abstract**—Novel metamaterial structures featuring left-handed (LH) and composite right/left-handed (CRLH) character are presented. The proposed unit cells utilize sections of coupled transmission lines. It is shown that by taking advantage of the coupling between transmission lines an additional degree of freedom is achieved, and therefore, the design process of artificial transmission lines is more flexible. The general behavior of each of the proposed circuits is presented and analyzed. Moreover, the design equations are formulated and the design process of each unit cell is described. The usefulness and validity of the proposed unit cells are illustrated and verified by the design and measurements of compact artificial transmission line sections utilizing the presented structures. Moreover, possible applications are discussed.

**Index Terms**—Artificial transmission lines, coupled-line sections, composite right/left-handed (CRLH), left-handed (LH) unit cell, metamaterials.

## I. INTRODUCTION

**I**N RECENT years, the left-handed (LH) metamaterials, first theoretically proposed by Veselago [1], have gained a significant interest. The possibility of realization of metamaterials for microwave applications has been a subject of extensive research. Although there are no homogeneous materials having left-handed properties, circuits featuring LH character in microwave frequency range have been developed.

The transmission-line approach to metamaterials has been introduced in [2] and [3]. In [4]–[6], the authors have investigated the possibility of realization of effectively homogenous (unit cell size much smaller than  $\lambda_g/4$ ) transmission lines featuring LH character which can be easily utilized in microwave applications. The authors have presented the structure realized as a finite number of periodically arranged unit cells composed of series capacitors and shunt inductors. Additionally, the authors have described the properties of such a unit cell, which in contrary to the previously presented resonant structures, e.g., [7], features broadband operation. However, the

Manuscript received September 09, 2014; revised November 07, 2014 and November 28, 2014; accepted November 30, 2014. Date of publication December 18, 2014; date of current version February 03, 2015. This work was supported in part by the National Science Centre under Contract DEC-2011/01/D/ST7/00789 and in part by the statutory activity of AGH Department of Electronics.

The authors are with the AGH University of Science and Technology, 30-059 Cracow, Poland (e-mail: jakub.sorocki@agh.edu.pl; ilona.piekarz@agh.edu.pl; krzysztof.wincza@agh.edu.pl; slawomir.gruszczyński@agh.edu.pl).

Color versions of one or more of the figures in this paper are available online at <http://ieeexplore.ieee.org>.

Digital Object Identifier 10.1109/TMTT.2014.2378283

ideal  $L$  and  $C$  elements are not physically realizable and the realized  $L$  and  $C$  equivalents feature unwanted parasitic effects in microwave frequency range. In [8], the structure has been described being a composite right/left-handed (CRLH) transmission line in which the parasitic series  $L$  and shunt  $C$  elements have been included and the need for modeling these effects has been shown. Since then, different models and realizations of the unit cells have been proposed taking into account parasitic effects or taking advantage of them [9]–[11]. One of the solutions is the utilization of transmission lines or coupled-lines as unit cell elements. Attempts to incorporate coupled-line sections into the design of LH unit cells have been a subject of several papers. In [12], Abdelaziz *et al.* have proposed the CRLH unit cell composed of two coupled-line sections in shorted-open-shorted (SOS) and open-shorted-open (OSO) configurations. In [13] and [14], the authors have presented unit cells based on Schiffman “C” section-like structures which feature LH character when the appropriate electrical length of a coupled-line section is selected.

Also multiconductor transmission-line-based stubs have been investigated in order to realize an appropriate shunt impedance, or multi-finger structures which in specific frequency range can act as appropriate series and shunt impedances allowing to realize unit cells having composite right/left-handed character [15], [16]. However, in the mentioned structures a complicated technology process (bonding) is needed.

In this paper, we present novel unit cells featuring LH character in a specified frequency range composed of coupled transmission line sections. Three novel unit cells are introduced and analyzed, i.e.: 1) a unit cell composed of section of short-ended coupled-lines with series capacitor; 2) a unit cell with short-ended and open-ended coupled-line sections; and 3) a unit cell composed of section of short-ended coupled lines with series capacitor and transmission line sections featuring composite right/left-handed character. Moreover, it is shown that the latter can be balanced by adjusting the length of series transmission-line section. It is shown that the coupling between adjacent shorted transmission lines included into the design process gives an additional degree of freedom, and therefore, one can independently engineer bandwidth, impedance match as well as the shape of the dispersion characteristic, which makes the proposed structures flexible. Moreover, such an approach allows for obtaining very compact structures. The proposed unit cells can find applications in two basic types of circuits:

- In circuits and systems where an exact phase shift introduced by the unit cell/transmission line section at specified

frequency within passband is needed and the possibility of design and control the phase shift is crucial as in, e.g., [17] and [18]. Therefore, the proposed in Sections II-A and II-B LH unit cells can be very convenient.

- In circuits where broadband operation is needed. For this type, balanced CRLH unit cells where the transition between the left- and right-handed band is continuous can be applied as in [19]–[22], where broadband bandpass filters have been described. For such applications it is important to have an appropriate circuit model valid for broad frequency range to describe the behavior of the circuit. A unit cell proposed and described in Section II-C is well suitable for such an application. The unit cell is modeled mostly using distributed elements, in contrary to [19], which allows to keep the model simple and to include all important effects occurring in the structure. Additionally, the bandwidth of the proposed unit cell can be very wide as well as can be controlled in a very wide frequency range during the design process.

All the discussed unit cells are theoretically investigated and their behavior and properties are described and illustrated in Section II. Furthermore, the design formulas for each structure are formulated and general design procedure is described. Exemplary realizations of artificial transmission lines with left and right-/left-handed behavior composed of the proposed unit cells are presented in Section III together with their measurement results. Moreover, practical applications with the example of compact broadband bandpass filters are discussed in Section IV.

## II. UNIT CELLS ANALYSIS

The properties of a transmission line can be elaborated by the analysis of the ABCD matrix of its unit cell. For simple unit cells this method is easy to utilize, however when the unit cell becomes more complex, the ABCD matrix approach requires tedious calculations. An alternative method has been presented in [23], where Eberspacher and Eibert have proposed the analysis of a symmetric unit cell with the use of even and odd mode excitations. Such a method simplifies the calculations by decomposition of the considered structure into two sub-networks, described by even  $Z_e$  and odd  $Z_o$  impedances, which are less complex than the ones obtained for the initial network. The important properties of unit cells, i.e., propagation constant, pass band limits and Bloch impedance, can be determined from these impedances.

The propagation constant can be derived from

$$\cosh(\gamma p) = \cosh(\alpha p + j\beta p) = A = \frac{Z_e + Z_o}{Z_e - Z_o} \quad (1)$$

where  $A$  is parameter of ABCD matrix [24]. For lossless case, the unattenuated operation is possible only for  $-1 \leq A \leq 1$  and operating band limits (cutoff frequencies) can be calculated by solving  $A(\omega) = \pm 1$  or by finding poles or zeroes of  $Z_e$  and  $Z_o$  as proposed in [18], hence

$$A = +1 : Z_e = \infty \vee Z_o = 0 \quad (2a)$$

$$A = -1 : Z_e = 0 \vee Z_o = \infty. \quad (2b)$$

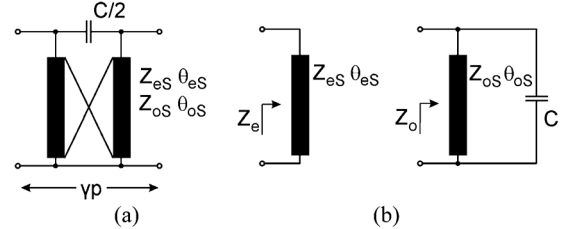


Fig. 1. (a) Equivalent circuit model of the proposed ideal LH transmission line unit cell composed of shorted coupled-line section and a lumped capacitor and (b) its decomposition into even and odd mode circuits.

The Bloch impedance equals

$$Z_B = \sqrt{-\text{Im}(Z_o)\text{Im}(Z_e)} \quad (3)$$

and within the passband is purely real.

The above presented method has been utilized to investigate the properties of novel unit cells. Moreover, to provide more general insight into the proposed unit cells (described in Sections II-A and II-C), they have been analyzed assuming that modal phase velocities occurring in a coupled-line section may be different. A parameter  $u$  describing this difference has been defined as

$$u = \frac{v_{po} - v_{pe}}{v_{po} + v_{pe}} = \frac{\sqrt{\epsilon_{effe}} - \sqrt{\epsilon_{effo}}}{\sqrt{\epsilon_{effe}} + \sqrt{\epsilon_{effo}}} \quad (4)$$

where  $\epsilon_{effe}$  is even and  $\epsilon_{effo}$  is odd mode effective permittivity having relation with phase velocities being  $v_{pe} = c/\sqrt{\epsilon_{effe}}$  and  $v_{po} = c/\sqrt{\epsilon_{effo}}$  ( $c$  is a free space velocity of light). Therefore, the formulated design equations for each considered structure can be successfully applied for inhomogenous (microstrip) structures where  $u \neq 0$  as well as for homogenous (stripline) structures where  $u = 0$  as in case of the unit cell described in Section II-B.

### A. Left-Handed Unit Cell Composed of Short-Ended Coupled-Line Section and Series Capacitor

An ideal left-handed transmission line unit cell can be composed of series capacitor and shunt inductor [4]. However, in practical realization there are always parasitic effects occurring which influence the performance of the circuit. It is then justify to research new circuits incorporating parasitics and allowing for better modeling of the existing phenomena. Since short-ended section of a transmission line has within the restricted frequency range an inductive character, it is worth considering a unit cell composed of two such elements with series capacitor, as it has been shown in [7]. However, in many practical applications, the coupling between adjacent inductors/transmission lines is unavoidable. Therefore, it is worth investigating the influence of the mutual coupling of the short-ended coupled lines on the dispersion characteristic of the artificial transmission line composed of unit cells shown in Fig. 1(a).

In the presented approach, one can take an advantage of the coupling and by controlling the spacing between lines one can modify the dispersion curve. Such an approach introduces an additional degree of freedom in a form of coupling level to the design of a LH unit cell, allowing for a separate design of

bandwidth, Bloch impedance and dispersion characteristic (i.e., phase shift  $\Delta\phi_0$  introduced by unit cell at  $f_0$ ).

The proposed unit cell has been analyzed assuming that the modal phase velocities occurring in a coupled-line section may differ. The even and odd mode impedances of the proposed unit cell [see Fig. 1(b)] can be calculated as:

$$Z_e = jZ_{eS} \tan(\theta_{eS}) \quad (5)$$

$$\begin{aligned} Z_o &= jZ_{oS} \tan(\theta_{oS}) \| -jX_C \\ &= j \frac{Z_{oS} \tan(\theta_{oS})}{1 - \omega C Z_{oS} \tan(\theta_{oS})} \end{aligned} \quad (6)$$

where  $\theta_{eS} = (f/f_0)\theta_{0eS}$ ,  $\theta_{oS} = (f/f_0)\theta_{0oS}$  and  $\theta_{0eS}, \theta_{0oS}$  are the modal electrical lengths of short-ended coupled-line section defined at  $f_0$  ( $f_{coL} < f_0 < f_{coH}$ ,  $f_{coL}$  and  $f_{coH}$  are lower and upper cutoff frequencies, respectively). The unit cell features periodical bandpass character but we investigate only the lowest order band.

As it has been presented, the band limits are determined by poles of  $Z_o$  and  $Z_e$

$$Z_{eS} \tan\left(\frac{f_{coH}}{f_0}\theta_{e0S}\right) \rightarrow \infty \quad (7)$$

$$1 - \omega_{coL} C Z_{oS} \tan\left(\frac{f_{coL}}{f_0}\theta_{0oS}\right) = 0. \quad (8)$$

For the proposed structure, the Bloch impedance equals

$$Z_B = \sqrt{\frac{-Z_{eS} \tan(\theta_{eS}) Z_{oS} \tan(\theta_{oS})}{1 - 2\pi f C Z_{oS} \tan(\theta_{oS})}}. \quad (9)$$

In the proposed unit cell, there are five variables ( $Z_{eS}$ ,  $Z_{oS}$ ,  $\theta_{0eS}$ ,  $\theta_{0oS}$ , and  $C$ ) and five design parameters ( $f_{coH}$ ,  $f_{coL}$ ,  $Z_B @ f_0$ ,  $\Delta\phi_0$ , and  $u$ ), therefore, independent selection of each parameter is possible. A single unit cell introduces at  $f_0$  phase shift equal [see (10) at the bottom of the page].

For small  $\Delta\phi_0$ , to calculate the introduced phase shift an approximation of arctangent function  $\arctan(k) \approx k$  can be used yielding an error lower than  $1^\circ$  for  $k$  smaller than  $20^\circ$  (see the appendix). For larger angles, the correction must be done by slight tuning of  $Z_{eS}$ . By combining (7)–(10) and using the previously mentioned approximation, the values of the elements can be calculated as

$$\theta_{0eS} = \frac{f_0}{f_{coH}} \frac{\pi}{2} \quad (11)$$

$$\theta_{0oS} = \frac{(1-u)}{(1+u)} \theta_{0eS} \quad (12)$$

$$Z_{eS} \approx \frac{Z_B}{\tan(\theta_{0eS})} \sqrt{\frac{\sqrt{(\Delta\phi_0^2 + 1)} + 1}{\sqrt{(\Delta\phi_0^2 + 1)} - 1}} \quad (13)$$

$$\begin{aligned} Z_{oS} &= \frac{Z_B^2}{Z_{eS} \tan(\theta_{0eS}) \tan(\theta_{0oS})} \\ &\times \left[ \frac{f_0}{f_{coL}} \cot\left(\frac{f_{coL}}{f_0}\theta_{0oS}\right) \tan(\theta_{0oS}) - 1 \right] \end{aligned} \quad (14)$$

$$C = \left( 2\pi f_{coL} Z_{oS} \tan\left(\frac{f_{coL}}{f_0}\theta_{0oS}\right) \right)^{-1}. \quad (15)$$

In case where shorted transmission lines of the proposed unit cell become uncoupled, hence  $Z_{eS} = Z_{oS} = Z_S$  we obtain a circuit similar to the well-known in literature unit cells composed of series capacitor and short ended stubs. By utilization of coupled-lines, one can realize the given phase shift using lines having lower impedance and smaller capacitor values in comparison to the well-known unit cell composed of uncoupled transmission lines at the expense of the bandwidth reduction. However, the lower phase shift is required for a given bandwidth, the greater coupling between lines is needed. Additionally, when a unit cell needs to be realized in inhomogenous structure, the bigger parameter  $u$  the greater increase of  $Z_{oS}$  value and  $C$  with respect to the case when  $u = 0$ . The parameter  $u$  also influences the location of higher-order passbands (see Fig. 2). The advantage of the unit cell is its more compact physical structure allowing for the reduction of occupied space in comparison to the one presented in literature [7], since there is no need to ensure that the short-ended lines are uncoupled, and therefore, the lines can be much closer to each other. Moreover, bandwidth and phase shift  $\Delta\phi_0$  as well as Bloch impedance can be chosen separately.

An exemplary set of characteristics of the proposed unit cell is presented in Fig. 2 assuming  $f_0 = 1.5$  GHz,  $f_{coL} = 1$  GHz,  $f_{coH} = 2$  GHz,  $Z_B = 50$  Ω, and  $\Delta\phi_{0\text{assumed}} = -30^\circ$  for two cases: 1)  $u = 0$  [see Fig. 2(a)–(c)] for which  $\theta_{0eS} = \theta_{0oS} = 67.5^\circ$ ,  $Z_{eS} = 84.2$  Ω,  $Z_{oS} = 13.35$  Ω,  $C = 11.9$  pF,  $\Delta\phi_0 = -27.6^\circ$  and 2)  $u = 0.05$  [see Fig. 2(d)–(f)] for which  $\theta_{0eS} = 67.5^\circ$ ,  $\theta_{0oS} = 61.07^\circ$ ,  $Z_{eS} = 84.2$  Ω,  $Z_{oS} = 14.64$  Ω,  $C = 12.6$  pF,  $\Delta\phi_0 = -27.6^\circ$ .

### B. Left Handed Unit Cell Based on Short- and Open-Ended Coupled-Line Sections

All realizations of LH unit cells shown in literature and in Section II-A put emphasis on substitution of lumped inductors by uncoupled or coupled short-ended transmission-line sections. However, the realization of lumped capacitors can also be problematic since the utilization of SMD components introduces parasitic reactances not fully taken into account in the design. Furthermore, the realization of between-layer capacitors as metallization pads on two sides of thin dielectric laminate also introduces parasitic inductance. Since the realization of all circuit components in PCB technology is highly desirable in many applications, it is worth considering a unit cell shown

$$\beta_0 p = \Delta\phi_0 = \text{Im} \left\{ \arccos h \left( \frac{-Z_{eS} \tan(\theta_{0eS}) Z_{oS} \tan(\theta_{0oS}) 2\pi f_0 C + Z_{eS} \tan(\theta_{0eS}) + Z_{oS} \tan(\theta_{0oS})}{-Z_{eS} \tan(\theta_{0eS}) Z_{oS} \tan(\theta_{0oS}) 2\pi f_0 C + Z_{eS} \tan(\theta_{0eS}) - Z_{oS} \tan(\theta_{0oS})} \right) \right\} \quad (10)$$

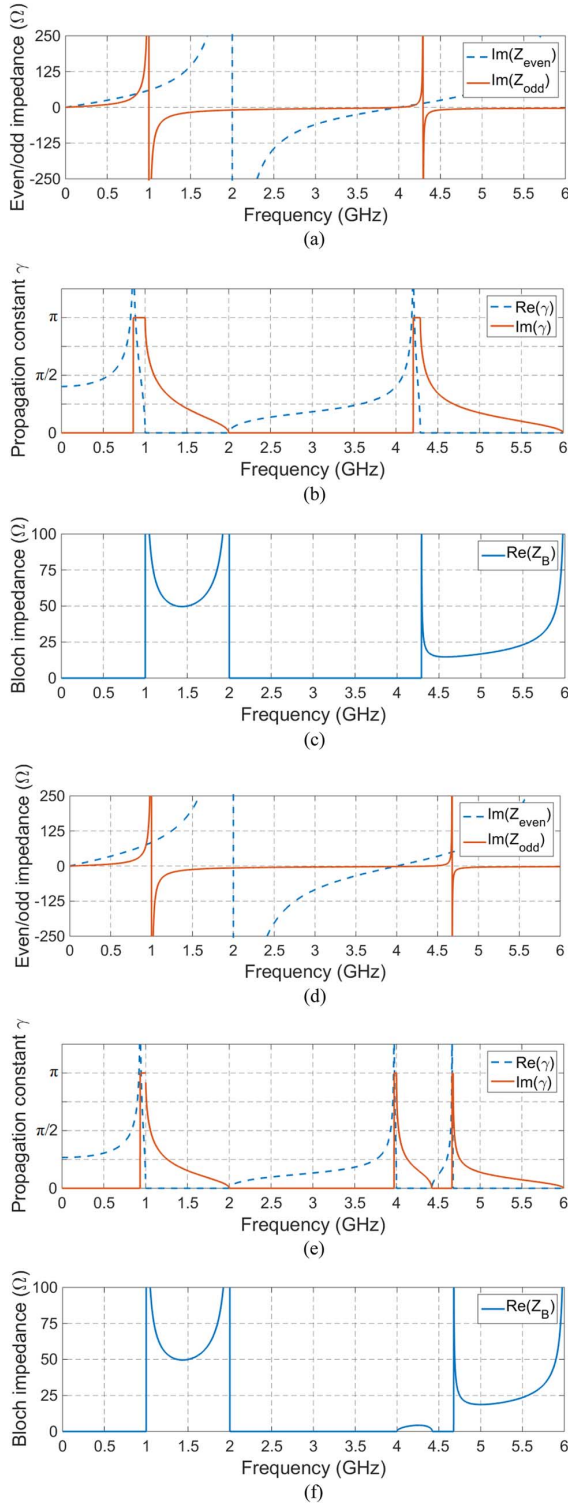


Fig. 2. (a) Imaginary parts of even- and odd-mode impedances, (b) real and imaginary part of propagation constant, and (c) real part of Bloch impedance of the proposed left-handed unit cell composed of ideal capacitor, and (d–f) shorted coupled-line section for  $u = 0$  and corresponding figures for  $u = 0.05$ .

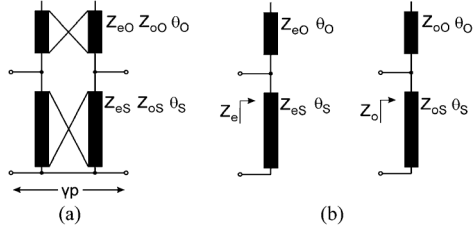


Fig. 3. (a) Equivalent circuit model of the proposed LH transmission-line unit cell composed of shorted and open-ended coupled-line sections and (b) its decomposition into even and odd mode circuits.

in Fig. 3(a) composed of short- and open-ended sections of coupled-lines having, within the restricted frequency range, inductive and capacitive character respectively. Such a structure may be very convenient to model and design, however a relatively strong coupling of open-ended coupled-line section is needed to ensure its proper behavior. It is then a natural choice to utilize multilayer stripline dielectric structures. Moreover, an advantage of such structures is that a problem of inequality of modal phase velocities does not occur, hence the analysis and design are simplified.

The proposed unit cell has been decomposed into even and odd circuits [see Fig. 3(b)] similarly to the previously shown unit cell. As seen, modal phase velocities are assumed to be equal.

The even and odd mode impedances [see Fig. 3(b)] can be calculated as

$$\begin{aligned} Z_e &= -jZ_{eo} \cot(\theta_O) \| jZ_{es} \tan(\theta_S) \\ &= j \frac{Z_{eo} \cot(\theta_O) Z_{es} \tan(\theta_S)}{Z_{eo} \cot(\theta_O) - Z_{es} \tan(\theta_S)} \end{aligned} \quad (16)$$

$$\begin{aligned} Z_o &= -jZ_{oo} \cot(\theta_O) \| jZ_{os} \tan(\theta_S) \\ &= j \frac{Z_{oo} \cot(\theta_O) Z_{os} \tan(\theta_S)}{Z_{oo} \cot(\theta_O) - Z_{os} \tan(\theta_S)} \end{aligned} \quad (17)$$

where  $\theta_S = (f/f_0)\theta_{0S}$  and  $\theta_{0S}$  is the electrical length of shorted coupled-line section and  $\theta_O = (f/f_0)\theta_{0O}$  and  $\theta_{0O}$  is the electrical length of open coupled-line section, both defined at  $f_0$  ( $f_{coL} < f_0 < f_{coH}$ ). Similarly to the previous case, despite the periodicity of the passband, only the lowest order band has been investigated and the band limits are determined by poles of  $Z_o$  and  $Z_e$ . For these conditions we have

$$Z_{eo} \cot\left(\frac{f_{coH}}{f_0} \theta_{0O}\right) - Z_{es} \tan\left(\frac{f_{coH}}{f_0} \theta_{0S}\right) = 0 \quad (18)$$

$$Z_{oo} \cot\left(\frac{f_{coL}}{f_0} \theta_{0O}\right) - Z_{os} \tan\left(\frac{f_{coL}}{f_0} \theta_{0S}\right) = 0. \quad (19)$$

The Bloch impedance of the proposed structure equals [see (20) at the bottom of the page].

$$Z_B = \sqrt{-\frac{Z_{eo} \cot(\theta_O) Z_{es} \tan(\theta_S)}{Z_{eo} \cot(\theta_O) - Z_{es} \tan(\theta_S)} \cdot \frac{Z_{oo} \cot(\theta_O) Z_{os} \tan(\theta_S)}{Z_{oo} \cot(\theta_O) - Z_{os} \tan(\theta_S)}}. \quad (20)$$

Recognizing the analogy with the case presented in Section II-A we can take  $Z_{eO}$  and  $Z_{oO}$  of open-ended coupled lines as constant values being related to the maximum realizable mutual capacitance in a given dielectric structure and the physical length of a given unit cell. Under these assumptions four variables remain ( $Z_{eS}$ ,  $Z_{oS}$ ,  $\theta_{0S}$ , and  $\theta_{0O}$ ) and there are four design parameters ( $f_{coH}$ ,  $f_{coL}$ ,  $Z_B @ f_0$ , and  $\Delta\phi_0 @ f_0$ ). A single unit cell at  $f_0$  introduces phase shift equal [see (21) at the bottom of the page].

By combining (18)–(21) and using approximation  $\tan(\theta_{0O}) \approx \theta_{0O}$  (based on Maclaurin series expansion), given that  $\theta_{0O}$  is a relatively small angle (error lower than  $0.1^\circ$  for  $\theta_{0O}$  smaller than  $10^\circ$ ), the values of elements constituting the unit cell can be calculated as follows:

$$\Delta\phi_0 \approx \frac{\sqrt{1 - S^2}}{S} \quad (22)$$

$$L = \frac{f_{coL}}{f_0} \tan\left(\frac{f_{coL}}{f_0}\theta_{0S}\right) \quad (23a)$$

$$M = \tan(\theta_{0S}) \quad (23b)$$

$$H = \frac{f_{coH}}{f_0} \tan\left(\frac{f_{coH}}{f_0}\theta_{0S}\right) \quad (23c)$$

$$S = \frac{Z_{eO}(L - M) + Z_{oO}(H - M)}{Z_{eO}(L - M) - Z_{oO}(H - M)} \quad (23d)$$

$$\theta_{0O} \approx \sqrt{-\frac{Z_{eO}Z_{oO}}{Z_B^2}} \frac{M^2}{(H - M)(L - M)} \quad (24)$$

$$Z_{eS} = Z_{eO} \cot\left(\frac{f_{coH}}{f_0}\theta_{0O}\right) \cot\left(\frac{f_{coH}}{f_0}\theta_{0S}\right) \quad (25)$$

$$Z_{oS} = Z_{oO} \cot\left(\frac{f_{coL}}{f_0}\theta_{0O}\right) \cot\left(\frac{f_{coL}}{f_0}\theta_{0S}\right). \quad (26)$$

However, the relation between  $\Delta\phi_0$  and  $\theta_{0S}$  is analytically unsolvable and in order to obtain the required phase shift introduced by the unit cell, the electrical length  $\theta_{0S}$  is selected based on the simplified relation (see the appendix) for  $\Delta\phi_0$  ( $\theta_{0S}$ ) given by (22) (for  $\Delta\phi_0 = 30^\circ$  error does not exceed  $3^\circ$ ).

In the presented unit cell, the series impedance is realized with the use of an open-ended coupled-line section substituting the required capacitance from the previous cases. The minimum achievable modal impedances  $Z_{eO}$  and  $Z_{oO}$ , which depend on the utilized dielectric structure and available space, are important factors having influence on the values of unit cell elements. For a constant phase shift introduced by one unit cell, constant  $Z_B$  at  $f_0$ , and constant  $Z_{eO}$ , the higher  $Z_{oO}$  the longer  $\theta_{0O}$  is required, but shorter  $\theta_{0S}$  and weaker coupling between shorted coupled-lines are needed.

The exemplary set of characteristics of the proposed unit cells for the assumed  $f_0 = 1.5$  GHz,  $f_{coL} = 1$  GHz,  $f_{coH} = 2$  GHz,  $Z_{B\text{assumed}} = 50 \Omega$ , and  $\Delta\phi_0 \text{ assumed} = -30^\circ$ ,

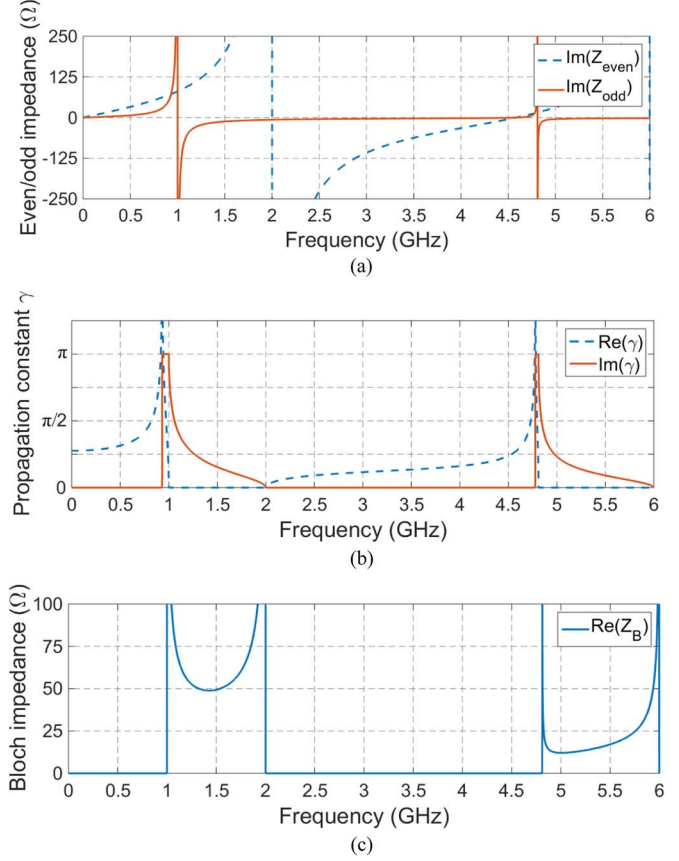


Fig. 4. (a) Imaginary parts of even- and odd-mode impedances, (b) real and imaginary part of propagation constant, and (c) real part of Bloch impedance of the proposed LH unit cell composed of open and shorted coupled-line sections.

$Z_{eO} = 92.18 \Omega$ ,  $Z_{oO} = 1.26 \Omega$  is shown in Fig. 4, for which  $\theta_{0S} = 58.9^\circ$ ,  $Z_{eS} = 90.52 \Omega$ ,  $Z_{oS} = 15.08 \Omega$ ,  $\theta_{0O} = 8.75^\circ$ ,  $Z_B = 48.83 \Omega$ ,  $\Delta\phi_0 = -27.7^\circ$ .

#### C. Balanced Composite Left/Right-Handed Unit Cell Based on Short-Ended Coupled-Line Section and Series Capacitor

It is required that the unit cell size  $p$  is significantly smaller than the quarter of guided wavelength at the center frequency in order to obtain purely left-handed properties. Otherwise, the electrical length of the connections will have influence on the dispersion properties and the unit cell will feature the properties of composite transmission line [8]. This influence can be modeled as a short section of transmission line in series with capacitor, transforming its impedance [see Fig. 5(a)]. It is then worth investigating the possibility of realization of a balanced composite right/left-handed unit cell by taking advantage of the existing short series TL section by extending it to the appropriate length. Moreover, similarly to the unit cell presented in Section II-A, the proposed unit cell has been analyzed assuming

$$\beta_0 p = \Delta\phi_0 = \text{Im} \left\{ \arccos h \left( \frac{Z_{eO}Z_{eS} [Z_{oO} \cot(\theta_{0O}) - Z_{oS} \cot(\theta_{0S})] + Z_{oO}Z_{oS} [Z_{eO} \cot(\theta_{0O}) - Z_{eS} \cot(\theta_{0S})]}{Z_{eO}Z_{eS} [Z_{oO} \cot(\theta_{0O}) - Z_{oS} \cot(\theta_{0S})] - Z_{oO}Z_{oS} [Z_{eO} \cot(\theta_{0O}) - Z_{eS} \cot(\theta_{0S})]} \right) \right\}. \quad (21)$$

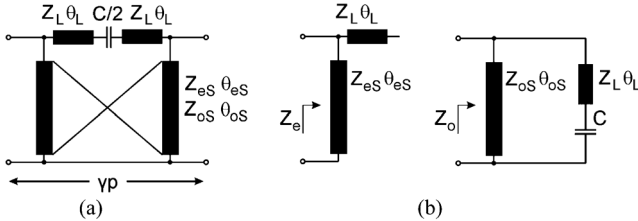


Fig. 5. (a) Equivalent circuit model of the considered composite left/right-handed transmission-line unit cell composed of short-ended coupled-line section and lumped capacitor and (b) its decomposition into even and odd mode circuits.

that modal phase velocities occurring in a coupled-line section may be different. The proposed structure has been decomposed into even and odd mode circuits [see Fig. 5(b)] and the even and odd mode impedances equal

$$Z_e = -j Z_L \cot(\theta_L) \| j Z_{eS} \tan(\theta_{eS}) \\ = j \frac{Z_L \cot(\theta_L) Z_{eS} \tan(\theta_{eS})}{Z_L \cot(\theta_L) - Z_{eS} \tan(\theta_{eS})} \quad (27)$$

$$Z_o = Z_L \frac{-j X_C + j Z_L \tan(\theta_L)}{Z_L + X_C \tan(\theta_L)} \| j Z_{oS} \tan(\theta_{oS}) \\ = j \frac{Z_{oS} \tan(\theta_{oS}) Z_L [Z_L \tan(\theta_L) - X_C]}{Z_{oS} \tan(\theta_{oS}) [Z_L + X_C \tan(\theta_L)] + Z_L [Z_L \tan(\theta_L) - X_C]} \quad (28)$$

where  $\theta_{eS} = (f/f_T)\theta_{0eS}$ ,  $\theta_{oS} = (f/f_T)\theta_{0oS}$ , and  $\theta_{0eS}, \theta_{0oS}$  are the modal electrical lengths of short-ended coupled-line section,  $\theta_L = (f/f_T)\theta_{0L}$  and  $\theta_{0L}$  is the electrical length of uncoupled section, all defined at  $f_T$  and  $f_T$  is the transition frequency between left-handed and right-handed region for which  $\gamma = 0$ ,  $X_C = 1/(2\pi f C)$ .

The composite right-/left-handed structure is called balanced when there is no stopband between left-handed and right-handed band. In case of even and odd mode analysis this translates into the analysis of two impedances:  $Z_e(f)$  and  $Z_o(f)$ . The balancing condition is given by  $Z_e(f_T) \rightarrow \infty$  and  $Z_o(f_T) = 0$  [18]. Thus the denominator of  $Z_e$  and the numerator of  $Z_o$  must both be equal to zero at transition frequency  $f_T$ , hence

$$Z_L \cot(\theta_{0L}) - Z_{eS} \tan(\theta_{0eS}) = 0 \quad (29)$$

$$Z_{oS} \tan(\theta_{0oS}) Z_L \left[ Z_L \tan(\theta_{0L}) - \frac{1}{2\pi f_T C} \right] = 0. \quad (30)$$

The lower and upper cutoff band limit appear for  $Z_o(f_{co}) \rightarrow \infty$  which means that the denominator of  $Z_o$  must be equal 0 for  $f_{co}$ , where  $f_{co}$  is either lower or higher cutoff frequency

$$Z_{oS} \tan\left(\frac{f_{co}}{f_T} \theta_{0oS}\right) \left[ Z_L + \frac{1}{2\pi f_{co} C} \tan\left(\frac{f_{co}}{f_T} \theta_{0L}\right) \right] \\ + Z_L \left[ Z_L \tan\left(\frac{f_{co}}{f_T} \theta_{0L}\right) - \frac{1}{2\pi f_{co} C} \right] = 0. \quad (31)$$

The Bloch impedance of the proposed structure equals [see (32) at the bottom of the page]. However, the Bloch impedance has to be defined at the frequency  $f_B$  (within first passband) which is different than  $f_T$  since at  $f_T$  the function has its discontinuity. For the desired operating frequency range of the unit cell, i.e.,  $f_T, f_{co}$ , and for  $Z_B$  (defined at  $f_B$ ), the required parameters of the unit cell can be calculated [using (29)–(32)]

$$\theta_{0S} = \frac{f_T \pi}{f_S 2} \quad (33)$$

$$\theta_{0eS} = \theta_{0S}(1+u) \quad \theta_{0oS} = \theta_{0S}(1-u) \quad (34)$$

$$D = \frac{\tan\left(\frac{f_B}{f_T} \theta_{0oS}\right) \left[ \tan\left(\frac{f_{co}}{f_T} \theta_{0L}\right) - \frac{f_T}{f_{co}} \tan(\theta_{0L}) \right]}{\tan\left(\frac{f_{co}}{f_T} \theta_{0oS}\right) \left[ 1 + \frac{f_T}{f_{co}} \tan(\theta_{0L}) \tan\left(\frac{f_{co}}{f_T} \theta_{0L}\right) \right]} \quad (35a)$$

$$E = \tan\left(\frac{f_B}{f_T} \theta_{0L}\right) - \frac{f_T}{f_B} \tan(\theta_{0L}) \quad (35b)$$

$$F = \cot\left(\frac{f_B}{f_T} \theta_{0L}\right) - \tan\left(\frac{f_B}{f_T} \theta_{0eS}\right) \cot(\theta_{0eS}) \cot(\theta_{0L}) \quad (35c)$$

$$G = 1 + \frac{f_T}{f_B} \tan(\theta_{0L}) \tan\left(\frac{f_B}{f_T} \theta_{0L}\right) \quad (35d)$$

$$H = \tan\left(\frac{f_B}{f_T} \theta_{0eS}\right) \cot(\theta_{0eS}) \cot\left(\frac{f_B}{f_T} \theta_{0L}\right) \cot(\theta_{0L}) \quad (35e)$$

$$Z_L = Z_B \sqrt{\frac{F(E - DG)}{DEH}} \quad (36)$$

$$Z_{eS} = Z_L \cot(\theta_{0L}) \cot(\theta_{0eS}) \quad (37)$$

$$Z_{oS} = -Z_L D \cot\left(\frac{f_B}{f_T} \theta_{0oS}\right) \quad (38)$$

$$C = (Z_L \tan(\theta_{0L}) 2\pi f_T)^{-1} \quad (39)$$

where  $f_S$  is the frequency at which  $\theta_{0S}$  equal  $\pi/2$ . The cutoff frequency  $f_{co}$  can be either lower or higher than  $f_T$ , and only one can be engineered. The second one  $f_{co2}$  results from the selection of  $f_S$ , however the relationship between  $f_S$  and  $f_{co2}$  cannot be analytically derived. For  $f_{co} < f_T$  the increase of  $f_B$  increases the bandwidth whereas for  $f_{co} > f_T$  decreases it. In order to maintain the balanced composite character and ensure physical realization of the unit cell, the conditions  $f_S > f_T$  as well as  $Z_{eS} > Z_{oS}$  must hold. Moreover, the electrical length  $\theta_{0L}$  gives an additional degree of freedom which can be used to adjust coupling  $k_S$  between coupled lines while maintaining the assumed bandwidth and Bloch impedance. The transmission line electrical length can be adjusted between minimum length required to operate in balanced mode and maximum value where coupled-lines become uncoupled (the longer  $\theta_{0L}$ , the lower coupling). Moreover, the influence of uneven modal electrical lengths ( $u \neq 0$ ) can be compensated by changing the electrical length of uncoupled series transmission lines.

$$Z_B = \sqrt{-\frac{Z_L \cot(\theta_L) Z_{eS} \tan(\theta_{eS})}{Z_L \cot(\theta_L) - Z_{eS} \tan(\theta_{eS})} \cdot \frac{Z_{oS} \tan(\theta_{oS}) Z_L [Z_L \tan(\theta_L) - X_C]}{Z_{oS} \tan(\theta_{oS}) [Z_L + X_C \tan(\theta_L)] + Z_L [Z_L \tan(\theta_L) - X_C]}}. \quad (32)$$

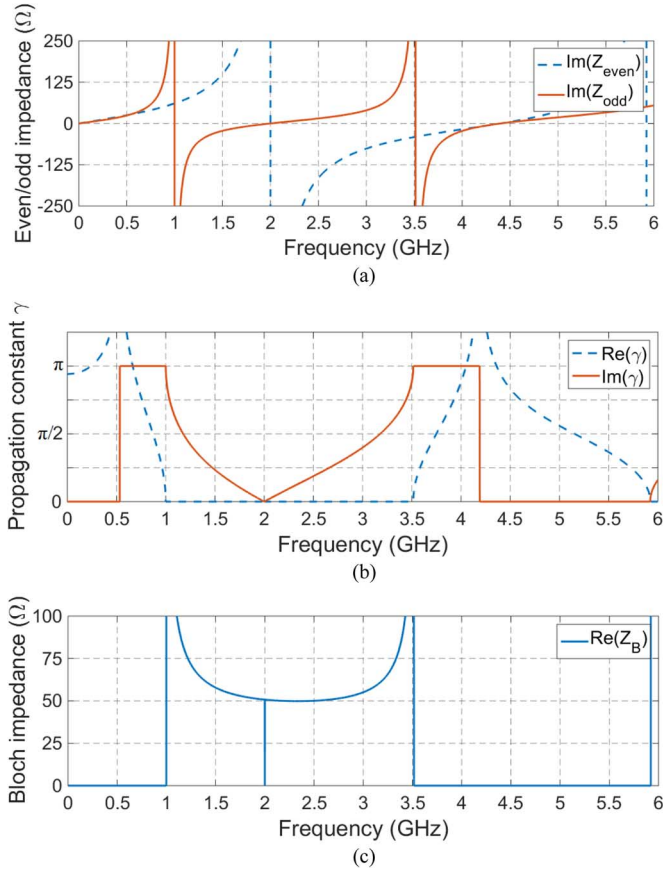


Fig. 6. (a) Imaginary parts of even- and odd-mode impedances real and (b) imaginary part of propagation constant and real part of Bloch impedance of the proposed balanced right/left-handed unit cell composed of a capacitor in series with short sections of transmission line and shorted coupled-line sections.

The exemplary set of characteristics of the proposed unit cell for  $f_T = 2 \text{ GHz}$ ,  $f_{co} = 1 \text{ GHz}$ ,  $f_B = 2.2 \text{ GHz}$ ,  $Z_B = 50 \Omega$ ,  $f_S = 2.2 \text{ GHz}$ , and  $\theta_{0L} = 15^\circ$ ,  $u = 0$ , what yields  $\theta_{0S} = 81.82^\circ$ ,  $Z_L = 122.8 \Omega$ ,  $Z_{eS} = 65.91 \Omega$ ,  $Z_{oS} = 53.53 \Omega$ ,  $C = 2.418 \text{ pF}$  are shown in Fig. 6.

### III. UNIT CELLS REALIZATION AND EXPERIMENTAL RESULTS

In order to experimentally verify the properties of the circuits proposed in previous sections, different transmission line sections composed of novel unit cells have been designed, manufactured, and measured. The physical realization allows for further integration of consecutive unit cells into more compact structures by realizing two parallel short-ended strips of coupled-line sections of adjacent unit cells as one, after the appropriate recalculation of strips' widths and spacing between coupled lines (see Fig. 7). The dimensions can be determined using, e.g., Linpar [25] based on per-unit-length capacitance matrix  $[C]$  describing single coupled-line section which is then recalculated into capacitance matrix  $[C']$  of multiconductor-coupled-lines. Having found short-ended coupled-line modal impedances from the derived design equations and knowing that

$$C_1 = \frac{1}{Z_{eS}v_{pe}} \quad C_m = 0.5 \left( \frac{1}{Z_{oS}v_{po}} - \frac{1}{Z_{eS}v_{pe}} \right) \quad (40)$$

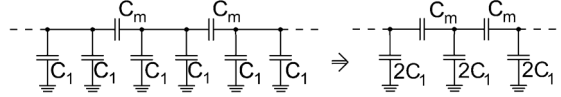


Fig. 7. Connection of  $[C]$  matrix elements of single shorted coupled-line section constituting unit cell to synthesize new multi-strip-coupled-line matrix  $[C']$ . In practical realization the consecutive metal strips of two adjacent unit cells can be realized as one.

one can calculate  $[C']$  as

$$\begin{aligned} C &= \begin{bmatrix} C_1 + C_m & -C_m \\ -C_m & C_1 + C_m \end{bmatrix} \Rightarrow C' \\ &= \begin{bmatrix} C_1 + C_m & -C_m & 0 & \dots & 0 \\ -C_m & 2C_1 + 2C_m & -C_m & \dots & 0 \\ 0 & -C_m & 2C_1 + 2C_m & \dots & 0 \\ \dots & \dots & \dots & \dots & -C_m \\ 0 & 0 & 0 & -C_m & C_1 + C_m \end{bmatrix} \end{aligned} \quad (41)$$

assuming that only adjacent lines are coupled and there are no losses (the size of the matrix equals  $n + 1$ ).

The applied design procedure can be formulated as follows.

- First, the design goals are defined, i.e.,  $f_{coL}$ ,  $f_{coH}$ ,  $f_0$ ,  $\Delta\phi_0$ , or  $f_{co}$ ,  $f_T$ ,  $Z_B$  and the number of subsections  $n$ . Moreover, the unit-cell topology and dielectric structure are selected based on system requirements.
- Second, the particular unit cell elements' values are calculated based on given in the previous sections design (11)–(15), (22)–(26), or (33)–(39).
- Next, the calculated parameters are confronted in terms of realization possibility in the chosen dielectric structure, and the physical dimensions of the elements are determined.
- In the next step, the dimensions of shorted multi-strip coupled-line integrating two adjacent unit cells' strips are calculated based on synthesized capacitive matrix  $[C']$ .
- Finally the structure is verified electromagnetically.

All the artificial transmission-line sections have been designed following the described procedure. Moreover, *AWR Microwave Office* software has been used for electromagnetic calculations.

It has to be underlined that an advantage of the proposed unit cells and the design approach is a significant reduction of circuit dimensions. The short-ended strips of consecutive unit cells are integrated into one and within the unit cell itself are coupled and close together in opposite to, e.g., [12]–[22], where the consecutive unit cells of artificial transmission lines or short-ended stubs are kept separated.

#### A. Artificial Transmission-Line Section—Example A

First, an artificial transmission line section has been designed based on the unit cell presented in Section II-A, referred as example A, in stripline dielectric structure shown in Fig. 8(a). having:  $f_{coL} = 0.3 \text{ GHz}$ ,  $f_{coH} = 1.1 \text{ GHz}$ ,  $f_0 = 0.7 \text{ GHz}$ ,  $Z_B@f_0 = 50 \Omega$ ,  $\Delta\phi_{0\text{assumed}} = -30^\circ$ . The circuit parameters have been found to be:  $Z_{eS} = 130.6 \Omega$ ,  $Z_{oS} = 54.93 \Omega$ ,

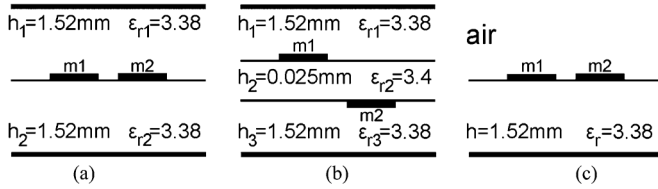


Fig. 8. Cross-sectional view of the dielectric structures utilized for the design of the presented examples. (a) Stripline, (b) multilayer stripline, and (c) single-layer microstrip.

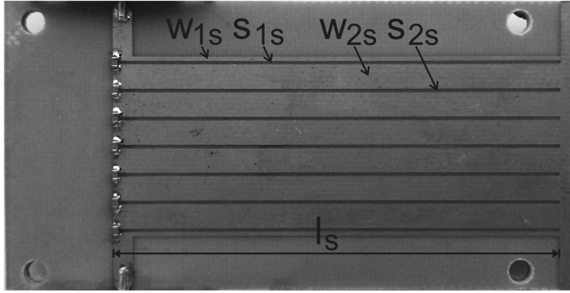


Fig. 9. Picture of the manufactured LH transmission line example A utilizing  $n = 7$  unit cells presented in Section II-A with top laminate removed. The dimensions are: width  $w_{1s} = 0.44\text{ mm}$ , spacing  $s_{1s} = 0.24\text{ mm}$ , width  $w_{2s} = 2.2\text{ mm}$ , spacing  $s_{2s} = 0.26\text{ mm}$ , length  $l_s = 39.3\text{ mm}$ . The overall size (not including signal lines) equals approximately  $93.3 \times 15.86\text{ mm}$ .

$\theta_{0S} = 57.57^\circ$ ,  $C/2 = 10.58\text{ pF}$ ,  $\Delta\phi_0 = -27.64^\circ$ . For series capacitance realization 10 pF 0402 SMD capacitors have been used what enforced slight circuit tuning. Moreover, SPICE model of a capacitor has been used for EM calculation. A picture of the manufactured circuit is presented in Fig. 9, whereas the measurement results in comparison with EM calculations are shown in Fig. 10.

As it can be seen, the measured lower cutoff slope is very sharp and corresponds to the slope of the theoretically calculated circuit. The measured phase shift per unit cell @  $f_0$  equals  $\Delta\phi_0 = -20.34^\circ$ . However, in physically realized structure, the response near the upper cutoff frequency is disturbed in comparison to the theoretical one. The proposed model of the unit cell does not fully describe the behavior of the circuit in higher frequency range since the physical length of the unit cell is not modeled (assumed 0).

#### B. Artificial Transmission-Line Section—Example B

In order to avoid problems related to the use of lumped capacitors a section denoted as example B has been designed, based on the unit cell presented in Section II-B. In this solution the lumped capacitor is replaced by an electrically short open-ended section of coupled lines. The additional advantage in this case is the possibility of the electromagnetic analysis of the entire section, where all parasitic effects are taken into account. The following parameters of the section have been selected:  $f_{coL} = 0.4\text{ GHz}$ ,  $f_{coH} = 1\text{ GHz}$ ,  $f_0 = 0.7\text{ GHz}$ ,  $Z_B@f_0 = 50\Omega$ . The dielectric structure utilized for the design is presented in Fig. 8(b). For open-ended coupled lines, the strip widths have been set to 2.5 with 0 mm offset and impedances  $Z_{eO}$  and  $Z_{oO}$  have been calculated to be  $Z_{eO} = 80.27\Omega$ ,  $Z_{oO} = 1\Omega$ . The  $\theta_{0S}$  has been chosen to result in  $\Delta\phi_0 \approx -30^\circ$  based

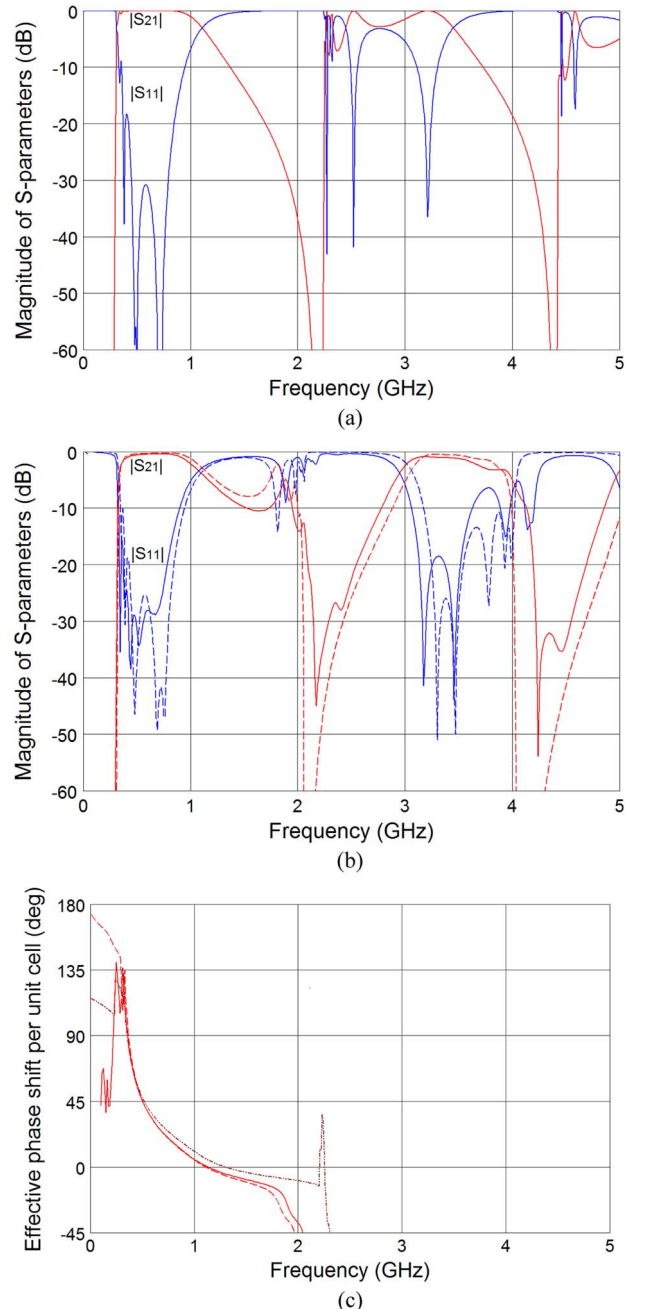


Fig. 10. (a) S-parameters of the manufactured transmission line example A calculated for ideal circuit composed of  $n = 7$  ideal unit cells and (b) EM calculated (dashed lines) in comparison with measured ones (solid lines). (c) De-embedded effective phase shift per unit cell  $\text{Ang}(S_{21})/n$ . Circuit analysis (dotted line), EM calculated (dashed line), and measured (solid line).

on (22). This yields the following element values:  $\theta_{0S} = 54.3^\circ$ ,  $Z_{eS} = 113.8\Omega$ ,  $Z_{oS} = 26.9\Omega$ ,  $\theta_{0O} = 6.19^\circ$ ,  $\Delta\phi_0 = -27.7^\circ$ . The picture of the manufactured circuit is presented in Fig. 11, whereas the measurement results are shown in Fig. 12.

As it can be seen, the developed example B features proper amplitude response up to the upper cutoff frequency of the fundamental band (good resemblance between circuit results, electromagnetic and measurement results up to the second passband). Also, the measured phase shift per unit cell @  $f_0$  equals  $\Delta\phi_0 = -23.51^\circ$  which is close to the designed value. Moreover, due to the realization of the LH section with distributed

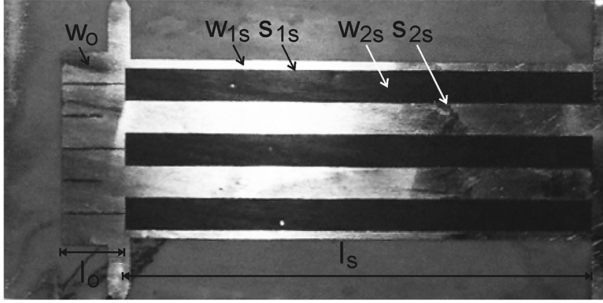


Fig. 11. Picture of the thin center laminate of the manufactured LH transmission line example B utilizing  $n = 6$  unit cell presented in Section II-D. The dimensions are: width  $w_O = 2.5$  mm, length  $l_O = 5$  mm, width  $w_{1s} = 0.66$  mm, spacing  $s_{1s} = 0.02$  mm (consecutive strips are on two sides of thin laminate), width  $w_{2s} = 2.52$  mm, spacing  $s_{2s} = 0.04$  mm, length  $l_S = 36.9$  mm. The overall size (not including signal lines) equals approximately  $42 \times 15.3$  mm.

elements only, the control over the parasitics is greater during the electromagnetic simulations than in the previous case.

### C. Artificial Composite Transmission-Line Section—Example C

In contrary to the LH lines presented previously, a balanced composite right/left-handed transmission line section with the use of coupled lines can be presented denoted as example C. The design is based on the unit cell presented in Section II-C and realized in stripline dielectric structure presented, in Fig. 7(a), hence the modal phase velocities are equal and  $u = 0$ . The following parameters have been chosen:  $f_{co} = 1$  GHz,  $f_T = 2$  GHz,  $f_B = 2.25$  GHz,  $Z_B @ f_B = 50 \Omega$ ,  $f_S = 2.25$  GHz. This yields the following element values:  $\theta_{0S} = 80^\circ$ ,  $Z_L = 110.6 \Omega$ ,  $\theta_{0L} = 11.3^\circ$ ,  $Z_{eS} = 97.6 \Omega$ ,  $Z_{oS} = 38.1 \Omega$  ( $k = 0.44$ ),  $C/2 = 1.8$  pF. The coupling between shorted lines has been optimized in order to obtain capacitance  $C/2$  being equal to the value of commercially available SMD capacitors. A picture of the manufactured circuit is presented in Fig. 13, whereas the measurement results are shown in Fig. 14.

As it can be seen, the lower and upper cutoff slope of the measured section corresponds to the results of the circuit calculations. The section is properly balanced, and no additional stop-band within the passband is introduced. The measured return losses are better than 15 dB over a wide frequency range. Also the periodicity of transmission line frequency characteristics is clearly visible.

### D. Artificial Composite Transmission-Line Section—Example D

The experimental example, denoted as example D of a balanced right/left-handed transmission line section composed of the composite unit cell presented in Section II-C has been realized in microstrip dielectric structure presented in Fig. 8(c). In this case the modal phase velocities of coupled-line section are unequal ( $u \neq 0$ ). Such a realization is very attractive for practical applications, since only a single-layer structure is needed. However, the design process is slightly more complicated. An iterative method can be proposed to calculate circuit elements

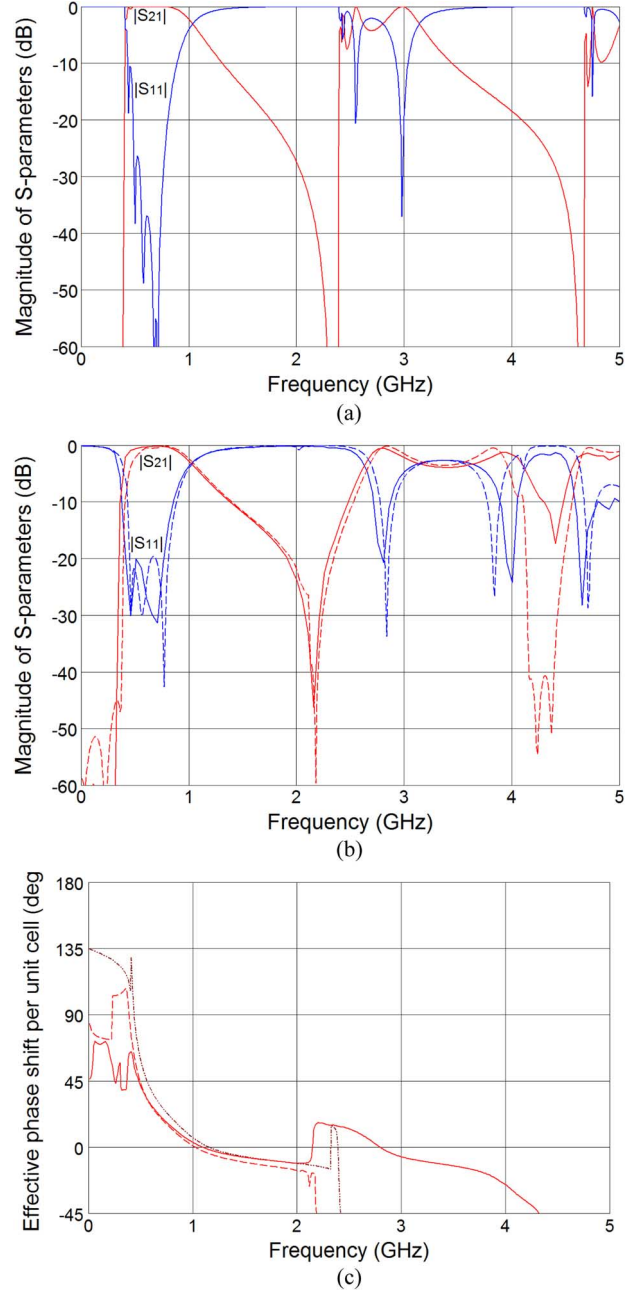


Fig. 12. (a) S-parameters of the manufactured transmission line example B calculated for ideal circuit composed of  $n = 6$  ideal unit cells and (b) EM calculated (dashed lines) in comparison with measured ones (solid lines). (c) De-embedded effective phase shift per unit cell  $\text{Ang}(S_{21})/n$ . Circuit analysis—dotted line, EM calculated—dashed line and measured—solid line.

since the modal effective permittivities are related to the coupled strip geometry and their change influences the initially calculated values. The following parameters have been chosen for the design of example D:  $f_{co} = 1$  GHz,  $f_T = 2$  GHz,  $f_B = 2.2$  GHz,  $Z_B @ f_B = 50 \Omega$ ,  $f_S = 2.2$  GHz while the effective permittivities are initially assumed to be  $\epsilon_{effe} = 2.5$ ,  $\epsilon_{effo} = 2.2$ ,  $u = 0.0319$ , and  $\theta_{0L} = 8.6^\circ$ . This yields the following element values:  $\theta_{0eS} = 84.43^\circ$ ,  $\theta_{0oS} = 79.2^\circ$ ,  $Z_L = 146.9 \Omega$ ,  $Z_{eS} = 94.68 \Omega$ ,  $Z_{oS} = 39.46 \Omega$  ( $k = 0.41$ ),  $C/2 = 1.8$  pF. Next, the capacitive matrix  $[C^t]$  is synthesized, based on which multi-strip coupled-line geometry can be found with, e.g., Linpar [25].

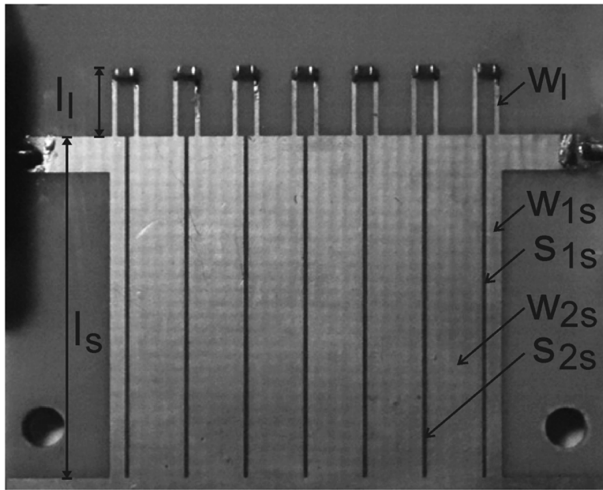


Fig. 13. Picture of the manufactured balanced composite right/left-handed transmission line example C utilizing  $n = 7$  unit cell presented in Section II-C with top laminate removed realized in stripline technique. The dimensions are: width  $w_L = 0.27$  mm, length  $l_L = 3.3$  mm, width  $w_{1s} = 0.79$  mm, spacing  $s_{1s} = 0.02$  mm, width  $w_{2s} = 2.68$  mm, spacing  $s_{2s} = 0.13$  mm, length  $l_s = 16.8$  mm. The overall size (not including signal lines) equals approximately  $21 \times 19$  mm.

Feedback information regarding  $\varepsilon_{\text{effe}}$  and  $\varepsilon_{\text{effo}}$  can be then taken from numerically calculated  $[\mathbf{C}_{\text{calc}}]$  and  $[\mathbf{C}'_{0\text{calc}}]$  matrices for a given coupled-line geometry which can be recalculated to  $[\mathbf{C}_{\text{calc}}]$  and  $[\mathbf{C}'_{0\text{calc}}]$  according to (41) and compared with the assumed values ( $[\mathbf{C}'_0]$  is a capacitive matrix for homogeneous air filled structure) [26]. If the new numerically found values of  $\varepsilon_{\text{effe}}$  and  $\varepsilon_{\text{effo}}$  are not in close agreement with the assumed ones, they are taken as input values for the next iteration, the unit cell parameters are recalculated, and the design steps are repeated. If the values are in close agreement, i.e.,  $|\varepsilon_{\text{effe}}^{(n-1)} - \varepsilon_{\text{effe}}^{(n)}| < \xi$  and  $|\varepsilon_{\text{effo}}^{(n-1)} - \varepsilon_{\text{effo}}^{(n)}| < \xi$  ( $n$ —number of iteration,  $\xi$ —convergence error, here assumed  $\xi = 0.1$ ) the procedure converges and the circuit can be verified by electromagnetic analysis. In case of the design of example D only two iterations have been sufficient. During EM calculations, slight circuit tuning may be done to optimize circuit performance since the SMD components are available with quantized values. The picture of the manufactured circuit is presented in Fig. 15, whereas the measurement results are shown in Fig. 16.

The manufactured example D features similar performance as example C with the exception of the transition frequency, which is slightly shifted down. The experimental results prove a high design flexibility of the proposed unit cell as well as its compactness and the possibility of realization in stripline and microstrip technique.

The presented measurement results of example A and B LH transmission-lines have confirmed that proposed in Section II-A and Section II-B unit cells are suitable for applications, where a specified phase shift is required. On the other hand, as it is seen, the example C and D CRLH transmission-lines can be considered as broadband bandpass filters. The design equations presented in Section II-C allow for the design of such filters based on the specified cutoff frequency, transition frequency and impedance match. The presented theoretical and measurement results confirm that wide-passband and high-selectivity filters can be obtained.

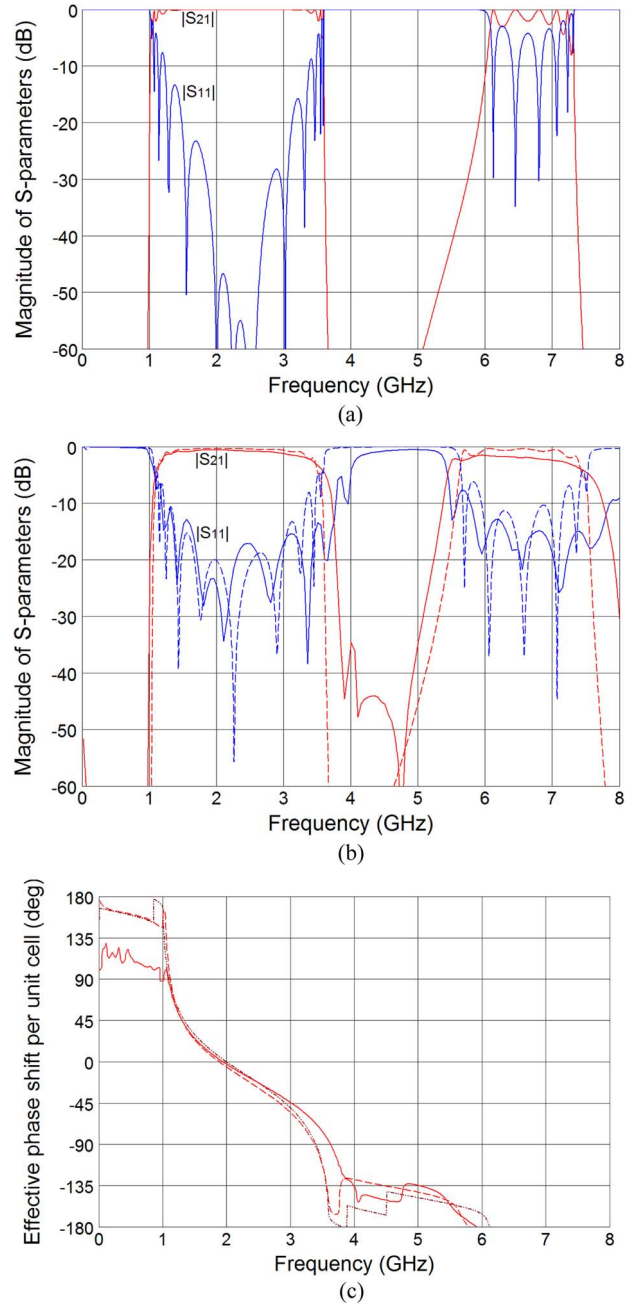


Fig. 14. (a) S-parameters of the manufactured transmission line example C calculated for ideal circuit composed of  $n = 7$  ideal unit cells and (b) EM calculated (dashed lines) in comparison with measured ones (solid lines). (c) De-embedded effective phase shift per unit cell  $\text{Ang}(S_{21})/n$ . Circuit analysis—dotted line, EM calculated—dashed line, and measured—solid line.

#### IV. RESULTS DISCUSSION IN CONTEXT OF FILTER APPLICATIONS

Since transmission-line sections composed of the proposed CRLH unit cells presented in Section II-C constitute broadband bandpass filters, it is worth to compare their performance with other proposed and described in literature composite metamaterial transmission-line based filters. As it can be seen from Table I, our proposed circuits are comparable in terms of bandwidth with the ones presented in [19] and [20]. However, in our solution single unit cell's size is much smaller than in the case of [19] and

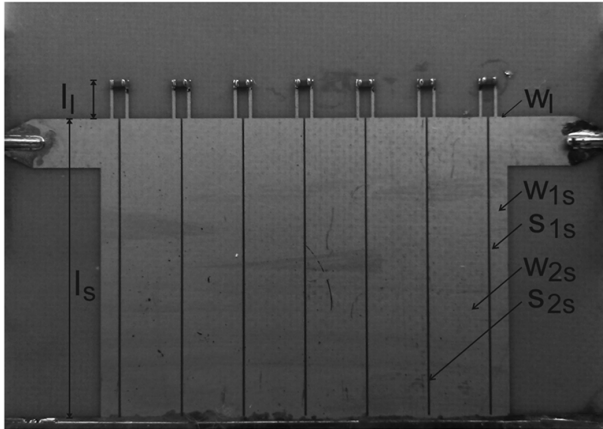


Fig. 15. Picture of the manufactured balanced composite right/left-handed transmission line example D utilizing  $n = 7$  unit cell presented in Section II-C realized in single-layer microstrip technique. The dimensions are: width  $w_L = 0.25$  mm, length  $l_L = 2.7$  mm, width  $w_{1s} = 1.3$  mm,  $s_{1s} = 0.1$  mm, width  $w_{2s} = 4.2$  mm, spacing  $s_{2s} = 0.1$  mm, length  $l_S = 21$  mm. The overall size (not including signal lines) equals approximately  $23.7 \times 28.5$  mm.

[20], and therefore, our artificial transmission line section composed of  $n = 7$  unit cells is comparable or even smaller than the artificial transmission lines presented in literature [19], [20] and composed of  $n = 3, 4, 1$  unit cells. It has to be noted, the higher  $n$  the greater out-of-band rejection and narrower transition band between pass and stopband, what is important in filter realization. Additionally, to realize the transmission line from [19] etching of two sides of PCB is required since the circuit utilizes the defected ground structure. The circuits proposed by us require only one side etching (example D) and an additional dielectric cover (example C), what simplifies the manufacturing process.

## V. CONCLUSION

Novel LH and composite right/left-handed unit cells have been proposed in this paper together with their theoretical analysis, design methodology and experimental verification. It is shown that the application of coupled transmission lines results in a very flexible design and allows for size reduction of the physically realized structure. It needs to be underlined that in the design of compact structures composed of distributed elements, the coupling between adjacent lines is unavoidable and, therefore, needs to be taken into account. Moreover, due to the use of coupled-lines, an additional degree of freedom is obtained which allows for independent design of bandwidth, impedance match and shape of the dispersion characteristic. Subsequently, it has been shown that an artificial transmission line composed of unit cells having short-ended coupled-line sections and series capacitors can be balanced by adding series electrically short transmission line sections. The exemplary sets of electrical parameters for each unit cell have been presented. The physical realizations and their measurement results proved the correctness of the presented analysis. The performance of each unit cell is also presented and discussed. Based on the presented results, one can choose the unit cell topology which is suitable for a given application.

## APPENDIX A

Arccosine hyperbolic function of  $x$  is calculated as

$$\arccos h(x) = \ln \left( x + \sqrt{x^2 - 1} \right). \quad (42)$$

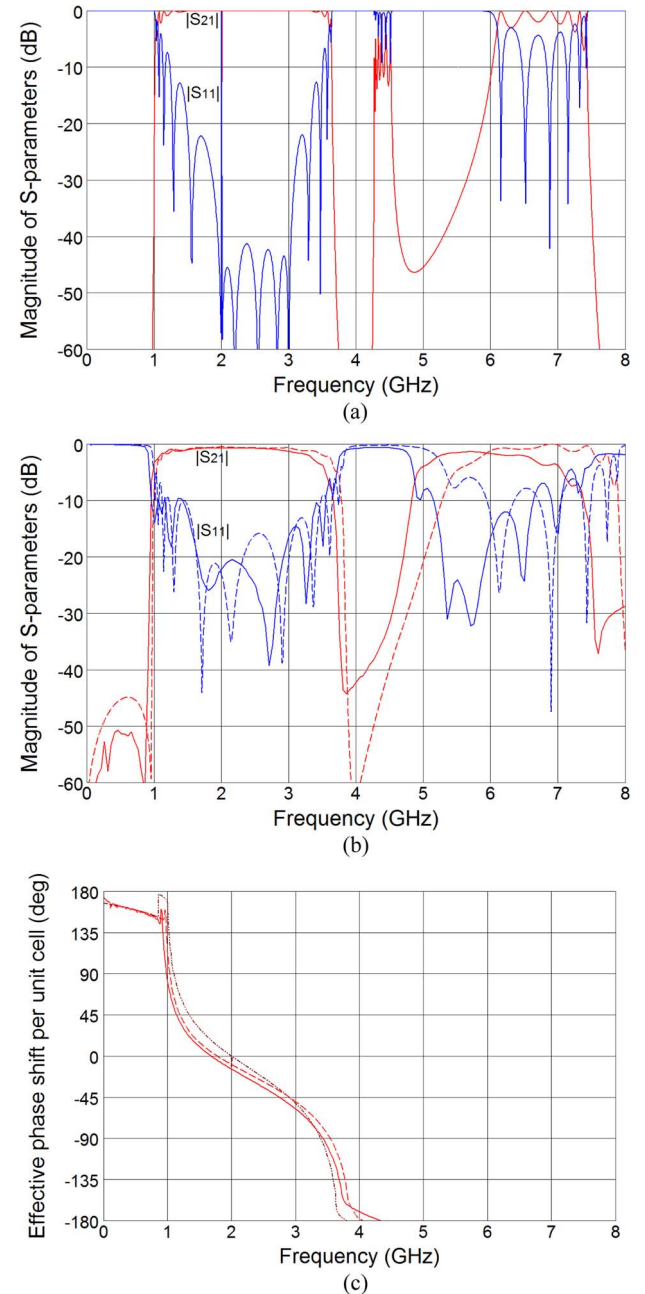


Fig. 16. (a) S-parameters of the manufactured transmission line example D calculated for ideal circuit composed of  $n = 7$  ideal unit cells (initial values of elements are used) and (b) EM calculated (dashed lines) in comparison with measured ones (solid lines). (c) De-embedded effective phase shift per unit cell  $\text{Ang}(S_{21})/n$ . Circuit analysis—dotted line, EM calculated—dashed line, and measured—solid line.

The natural logarithm of a complex number  $z$  is calculated as:  $\ln(z) = \ln(|z|) + j\angle(z)$ . The phase constant is the imaginary part of propagation constant, hence we need to calculate the  $\text{ang}(z)$  part of the logarithm. Within passband  $\sqrt{x^2 - 1}$  term is negative and  $x$  is a real number, hence

$$\beta_0 p = \Delta\phi_0 = \angle(x + j\sqrt{1 - x^2}) = \arctan(\sqrt{1 - x^2}/x). \quad (43)$$

TABLE I  
COMPARISON OF ARTIFICIAL TRANSMISSION LINE SECTIONS IN CONTEXT OF FILTERS REALISATION

	Bandwidth ( $f/f_T$ )	$n$	Size in $\lambda_g @ f_T$ for 50Ω TL	$f_T$ (GHz)	Realization
This paper, example C	3	7	0.258 x 0.233	2	stripline
This paper, example D	3.4	7	0.260 x 0.312	2	μstrip
[19], pure resonant approach	4.11	3	0.479 x 0.064	1	DG μstrip
[19], hybrid approach	2.86	4	0.657 x 0.235	5.5	DG μstrip
[20]	3.7	1	0.383 x 0.110	5	μstrip

The  $\arctan(k)$  function can be expanded into Maclaurin series as

$$\arctan(k) = k - \frac{k^3}{3} + \frac{k^5}{5} \dots = \sum_{n=0}^{\infty} \frac{(-1)^n k^{2n+1}}{2n+1} \quad (44)$$

for  $|k| \leq 1, k \neq \pm j$ .

## REFERENCES

- V. G. Veselago, "The electrodynamics of substances with simultaneously negative values of  $\epsilon$  and  $\mu$ ," *Soviet Phys. Uspekhi*, vol. 10, no. 4, pp. 509–514, Jan.–Feb. 1968.
- A. K. Iyer and G. V. Eleftheriades, "Negative refractive index metamaterials supporting 2-D waves," in *IEEE MTT-S Int. Microw. Symp. Dig.*, Seattle, WA, USA, Jun. 2–7, 2002, vol. 2, pp. 1067–1070.
- C. Caloz, H. Okabe, H. Iwai, and T. Itoh, "Transmission line approach of left-handed materials," in *USNC/URSI Nat. Radio Sci. Meet. Dig.*, San Antonio, TX, USA, Jun. 16–21, 2002, p. 39.
- G. V. Eleftheriades, A. K. Iyer, and P. C. Kremer, "Planar negative refractive index media using periodically L-C loaded transmission lines," *IEEE Trans. Microw. Theory Techn.*, vol. 50, no. 12, pp. 2702–2712, Dec. 2002.
- G. V. Eleftheriades, O. Siddiqui, and A. K. Iyer, "Transmission line models for negative refractive index media and associated implementations without excess resonators," *IEEE Microw. Wireless Compon. Lett.*, vol. 13, no. 2, pp. 1531–1539, Feb. 2003.
- C. Caloz and T. Itoh, "Transmission line approach of left-handed (LH) materials and microstrip implementation of an artificial LH transmission line," *IEEE Trans. Antennas Propag.*, vol. 52, no. 5, pp. 1159–1166, May 2004.
- R. A. Shelby, D. R. Smith, and S. Schultz, "Experimental verification of a negative index of refraction," *Science*, vol. 292, pp. 77–79, Apr. 2001.
- A. Lai, T. Itoh, and C. Caloz, "Composite right/left handed transmission line metamaterials," *IEEE Microw. Mag.*, vol. 5, no. 3, pp. 34–50, Sep. 2004.
- C. Caloz and T. Itoh, *Electromagnetic metamaterials: Transmission line theory and microwave applications*. Hoboken, NJ, USA: Wiley-IEEE Press, 2006.
- G. Eleftheriades and K. G. Balmain, *Negative-Refraction Metamaterials: Fundamental Principles and Applications*. Hoboken, NJ, USA: Wiley-IEEE Press, 2006.
- R. Marques, F. Martin, and M. Sorolla, *Metamaterials with Negative Parameters: Theory, Design, Microwave Applications*. Hoboken, NJ, USA: Wiley, 2008.
- A. F. Abdelaziz, T. M. Abuelfadil, and O. L. Elsayed, "Realization of composite right/left-handed transmission line using coupled lines," *Progr. Electromagn. Res. PIER*, vol. 92, pp. 299–315, 2009.
- A. M. E. Safwat, "Microstrip coupled line composite right/left-handed unit cell," *IEEE Microw. Wireless Compon. Lett.*, vol. 19, no. 7, pp. 434–436, Jul. 2009.
- J. Esteban, C. Camacho-Penalosa, J. E. Page, and T. M. Martin-Guerrero, "Generalized lattice network-based balanced composite right-/left-handed transmission lines," *IEEE Trans. Microw. Theory Techn.*, vol. 60, no. 8, pp. 2385–2393, Aug. 2012.
- J. J. Sanchez-Martinez, E. Marquez-Segura, and C. Camacho-Penalosa, "Analysis of wire-bonded multiconductor transmission-line-based stubs," *IEEE Trans. Microw. Theory Techn.*, vol. 61, no. 4, pp. 1467–1476, Apr. 2013.
- J. J. Sanchez-Martinez, E. Marquez-Segura, P. Otero, and C. Camacho-Penalosa, "Artificial transmission line with left/right-handed behavior based on wire bonded interdigital capacitors," *Progr. Electromagn. Res. B*, vol. 11, pp. 245–264, 2009.
- J. Sorocki, I. Piekarz, K. Wincza, and S. Gruszcynski, "Broadband magic-Ts with the use of coupled-line directional couplers and left-handed transmission line sections," *Int. J. RF Microw. Comput.-Aided Eng.*, vol. 24, no. 4, pp. 513–521, Jul. 2014.
- K. Staszek, J. Sorocki, P. Kaminski, K. Wincza, and S. Gruszcynski, "A broadband 3 dB tandem coupler utilizing right/left handed transmission line sections," *IEEE Microw. Wireless Compon. Lett.*, vol. 24, no. 4, pp. 236–238, Apr. 2014.
- M. Gil, J. Bonache, J. Garcia-Garcia, J. Martel, and F. Martin, "Composite right/left-handed metamaterial transmission lines based on complementary split-rings resonators and their applications to very wideband and compact filter design," *IEEE Trans. Microw. Theory Techn.*, vol. 55, no. 6, pp. 1296–1304, Feb. 2007.
- K. U. Ahmed and B. S. Virdee, "Ultra-wideband bandpass filter based on composite right/left handed transmission-line unit-cell," *IEEE Trans. Microw. Theory Techn.*, vol. 61, no. 2, pp. 782–788, Feb. 2013.
- S.-G. Mao, M.-S. Wu, Y.-Z. Chueh, and Ch. H. Chen, "Modeling of symmetric composite right/left-handed coplanar waveguides with applications to compact bandpass filters," *IEEE Trans. Microw. Theory Techn.*, vol. 53, no. 11, pp. 3460–3466, Nov. 2013.
- S. Karimian and Z. Hu, "Miniaturized composite right/left-handed stepped-impedance resonator bandpass filter," *IEEE Microw. Wireless Compon. Lett.*, vol. 22, no. 8, pp. 400–402, Aug. 2012.
- M. A. Eberspacher and T. F. Eibert, "Analysis of composite right/left-handed unit cells based on even-odd-mode excitation," *IEEE Trans. Microw. Theory Techn.*, vol. 60, no. 5, pp. 1186–1196, May 2012.
- D. M. Pozar, *Microwave engineering*, 3rd ed. Hoboken, NJ, USA: Wiley, 2005.
- A. R. Djordjevic, M. B. Bazdar, T. K. Sarkar, and R. F. Harrington, *Matrix Parameters for Multiconductor Transmission Lines*. Norwood, MA, USA: Artech House, 1990.
- J. Seigl, V. Tulaja, and R. Hoffman, *General Analysis of Interdigitated Microstrip Couplers*, ser. Siemens Forsch.-u. Entwickl.-Ber. Bd. 10, no. 4. Berlin, Germany: Springer-Verlag, 1981.



papers.

**Jakub Sorocki** received the M.Sc. degree in electronics and telecommunications from AGH University of Science and Technology, Cracow, Poland, in 2013, where he is currently pursuing the Ph.D. degree in electronics.

Since 2011 he has been cooperating with the Microwave Technology and High Frequency Electronics Research Team, Department of Electronics, AGH UST. His scientific research interests focus on left-handed metamaterials in microwave range. He has coauthored a few journals and conference



**Ilona Piekarz** received the M.Sc. degree in electronics and telecommunications from AGH University of Science and Technology, Cracow, Poland, in 2013, where she is currently pursuing the Ph.D. degree in electronics.

Since 2011 she has been cooperating with the Microwave Technology and High Frequency Electronics Research Team, Department of Electronics, AGH UST. She has coauthored a few journals and conference papers.

Miss Piekarz was a recipient of the received "Diamond Grant" for Outstanding Students awarded by the Ministry of Science and Higher Education for her research on microwave biosensors, in 2013.



**Sławomir Gruszczynski** (M'14) was born in Wrocław, Poland, on December 14, 1976. He received the M.Sc. and Ph.D. degrees in electronics and electrical engineering from the Wrocław University of Technology, Wrocław, Poland, in 2001 and 2006, respectively.

From 2001 to 2006, he has been with the Telecommunications Research Institute, Wrocław Division. From 2005 to 2009, he worked with the Institute of Telecommunications, Teleinformatics and Acoustics, Wrocław University of Technology. In 2009, he joined the Faculty of Informatics, Electronics and Telecommunications, AGH University of Science and Technology, where he became a Head of the Department of Electronics in 2012. He has coauthored 32 journal and 45 conference scientific papers.

Dr. Gruszczynski is a member of the Young Scientists' Academy, Polish Academy of Sciences (PAN) and Committee of Electronics and Telecommunications at Polish Academy of Sciences (PAN).



**Krzysztof Wincza** (M'11) was born in Walbrzych, Poland, on May 27, 1979. He received the M.Sc. and Ph.D. degrees in electronics and electrical engineering from the Wrocław University of Technology, Wrocław, Poland, in 2003 and 2007, respectively.

In 2007, he joined the Institute of Telecommunications, Teleinformatics, and Acoustics, Wrocław University of Technology. In 2009, he joined the Faculty of Electronics, AGH University of Science and Technology, where he became an Assistant Professor. He has coauthored 31 journal and 48 conference scientific papers.

Dr. Wincza was a recipient of The Youth Award presented at the 10th National Symposium of Radio Sciences (URSI) and the Young Scientist Grant awarded by the Foundation for Polish Science, in 2001 and 2008, respectively.